Gain-Scheduling Position Control Approaches for Electromagnetic Actuated Clutch Systems

Claudia-Adina Bojan-Dragos, Mircea-Bogdan Radac, Radu-Emil Precup, Elena-Lorena Hedrea, Alexandra-Iulia Szedlak-Stinean and Stefan Preitl

Department of Automation and Applied Informatics, Politehnica University Timisoara, Bd. V. Parvan 2, Timisoara, Romania

Keywords: Electromagnetic Actuated Clutch Systems, Gain-Scheduling Control, Nonlinear System, Simulation Results.

Abstract: The paper proposes three Gain-Scheduling (GS) control design approaches dedicated to the position control of electromagnetic actuated clutch systems. The initial nonlinear mathematical model of the plant is simplified and next linearized at six operating points to use it in the design approaches. Starting with classical Proportional-Integral (PI) controllers, three GS control versions, namely Lagrange, Cauchy and Switching GS, are next designed to ensure zero steady-state control error and the switching between PI controllers. All control solutions are tested and validated on the nonlinear model of the plant and a comparative analysis is included.

1 INTRODUCTION

The paper is focused on the development of three gain-scheduling control solutions (CSs) for electromagnetic actuated clutch systems (the plant) in the framework of electrically driven clutches which belong to vehicular power train system.

Several classical and modern control solutions for electromagnetic actuated clutch systems have been proposed recently including the following ones: two electromagnetic clutch water pumps that can control the coolant in terms of a nonlinear servo are designed in (Shin et al., 2013) using a model-free approach based on an online self-organizing adaptive fuzzy controller. A nonlinear feedforward–feedback control scheme is proposed in (Gao et al., 2014) to improve the performance of the position tracking control that consist of steady-state-like control, feedforward control based on reference dynamics, and state dependent feedback control. The design of an estimator for each clutch of the dual clutch transmission is carried out in (Oh et al., 2014) using shaft model-based observer, unknown input observers, and adaptive output torque observer. A position controller for a clutch actuator is suggested in (Losero et al., 2016) using a quasi-Linear Parameter Varying (LPV) Takagi-Sugeno representation and, in order to use unmeasured values in the controller, a Takagi-Sugeno switching observer. A parallel adaptive feedforward and bang-bang controller is proposed in (Temporelli et al., 2017) to control the clutch pressure with an electromechanical clutch actuator. A controller for an electromagnetic linear clutch actuator is given in (Ranjan et al., 2017).

Since linear controllers can usually ensure the CS performance specifications only in some neighbourhood of a single operating point, the Gain-Scheduling (GS) technique is popular as it generalizes the performance specifications over various operating points. An analysis of GS controllers which can vary slowly and can capture the plant's nonlinearities and the conditions which guarantee the stability using Lyapunov's stability theory, robustness and performance of the overall gain-scheduled design are given in (Shamma and Athans, 1990; Veselý and Ilka, 2013), with recent results outlined as follows: a Proportional-Integral (PI) GS CS for second-order LPV systems, which excludes time varying delay and uses a Smith predictor, is given in (Puig et al., 2012). GS deals in (Andonovski et al., 2015) with the adaptation of gains of a robust evolving cloud-based controller

Bojan-Dragos, C-A., Radac, M-B., Precup, R-E., Hedrea, E-L., Szedlak-Stinean, A-I. and Preitl, S.
Gain-Scheduling Position Control Approaches for Electromagnetic Actuated Clutch Systems.
DOI: 10.5220/0006900404110418
In *Proceedings of the 15th International Conference on Informatics in Control, Automation and Robotics (ICINCO 2018) - Volume 2*, pages 411-418
ISBN: 978-989-758-321-6

(RECCo) designed for a class of nonlinear processes; the robust modification of the adaptive laws and the performance analysis are introduced. A practical implementation of RECCo with normalized data space for a heat-exchanger plant is shown in (Andonovski et al., 2016). Other interesting GS (adaptive) control techniques for real practical applications are discussed in (Haidegger et al., 2012; Costa et al., 2015; Precup et al., 2015; Yang and Yan, 2016; Precup et al., 2017).

This paper continues with the modelling of a nonlinear electromagnetic actuator system in Section 2. Six linear PI controllers are designed in Section 3 based on the linearized mathematical models (MMs) of the plant. Three GS controllers are next suggested to ensure the switching between these linear PI controllers and to improve the performance indices. The parameters of the suggested controllers can be relatively easily adapted to the modifications of the operating points. The simulation results and comparisons between the suggested GS controllers are given in Section 4. Section 5 presents the conclusions.

2 MATHEMATICAL MODELING OF CONTROLLED PLANT

In this paper, the controlled plant is an electromagnetic actuator as part of a clutch system. The state-space MM of the electromagnetic actuated clutch is built around a magnetically actuated mass spring damper system, Figure 1 (Di Cairano et al., 2007). The mass m moves linearly under the effect of the magnetic force F, which is generated by the coil. Additional forces which acting on the mass are generated by the spring and the damper.

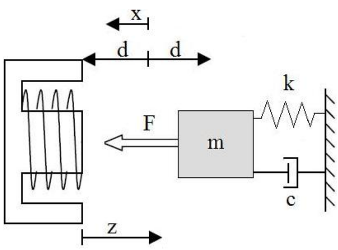

Figure 1: Schematic structure of the magnetically actuated mass-spring-damper system.

Using the equations given in (Di Cairano et al., 2007; Bishop, 2008), the dynamic behaviours of the mechanical (M-S) and electromagnetic subsystems (EM-S) are characterized by

$$\begin{aligned}(M-S):&\quad m\ddot{x}=F-c\dot{x}-kx\\ (EM-S):&\ \dot{\lambda}=V-Ri,\\ &\lambda=2k_a i/(k_b+d-x),\\ &F=k_a i^2/(k_b+d-x)^2=\lambda^2/(4k_a).\end{aligned}\tag{1}$$

Based on (1), the following simplified nonlinear state-space model of the plant can be accepted (Dragos et al., 2012a, Dragos et al., 2012b):

$$\begin{aligned}&\dot{x}_1=x_2,\\ &\dot{x}_2=-(k/m)x_1-(c/m)x_2+(k_a x_3^2)/[m(k_b\\ &+d-x_1)^2],\\ &\dot{x}_3=-[R(k_b+d-x_1)/(2k_a)]x_3-[1/(k_b\\ &+d-x_1)]x_2x_3+[(k_b+d-x_1)/(2k_a)]u,\\ &y=1000x_1,\end{aligned}\tag{2}$$

with the following characteristic variables: $u\in[0, 12]$ [V] is the control input, $x_1\in[0, 0.004]$ [m] is the mass position, x_2 [m/s] is mechanical subsystem's speed and $x_3=\lambda$ $[\mathrm{V\cdot s}]$ is the magnetic flux; y [m] is the output variable, i.e., the measured mass position, m=1 [kg] is the mass, d=0.004 [m] is the distance between contact position and spring neutral position, R=1.2 [Ω] is the resistance, c=700 [N s/m] coefficient of the damper, k=37500 [N/m] is stiffness of the spring, k_a=0.5 is a constant k_b=0.375 is a constant, $i\in[0, 10]$ [A] is the current, and $F\in[0, 150]$ [N] is the external magnetic force.

To design the proposed CS, the reduced model (2) is linearized at six operating points (o.p.s) with the following coordinates $P^{(j)}(x_1^{(j)},x_3^{(j)},u^{(j)})$, where j is the index of the current operating point, $j=\overline{1,6}$:

$$\begin{aligned}&P^{(1)}(0.002,5,6),P^{(2)}(0.0021,6,7.2),\\ &P^{(3)}(0.0023,7,8.4),P^{(4)}(0.0027,8,9.6),\\ &P^{(5)}(0.0033,9,10.8),P^{(6)}(0.0038,9.8,11.76).\end{aligned}\tag{3}$$

The simplified linearized state-space models (Ln-Ms) are

$$\begin{aligned}
&\Delta\dot{\mathbf{x}}^{(j)} = \mathbf{A}^{(j)}\,\Delta\mathbf{x}^{(j)} + \mathbf{b}^{(j)}\,\Delta u^{(j)},\\
&\Delta y^{(j)} = \mathbf{c}^{T(j)}\,\Delta\mathbf{x}^{(j)}\\
&\Delta\mathbf{x}^{(j)} = \left[\Delta x_1^{(j)} \quad \Delta x_2^{(j)} \quad \Delta x_3^{(j)}\right]^T,\\
&\Delta\mathbf{x}^{(j)} \in \Re^{3x1},\ \Delta u^{(j)} \in \Re,\\
&\mathbf{A}^{(j)} = \begin{bmatrix} 0 & 1 & 0\\ a_{21}^{(j)} & a_{22}^{(j)} & a_{23}^{(j)}\\ 0 & a_{32}^{(j)} & a_{33}^{(j)} \end{bmatrix}, \mathbf{b}^{(j)} = \begin{bmatrix} 0\\ 0\\ k_b/(2k_a) \end{bmatrix},\\
&\mathbf{c}^{T(j)} = [1000 \quad 0 \quad 0],\\
&\mathbf{A}^{(j)} \in \Re^{3x3},\ \mathbf{b}^{(j)} \in \Re^{3x1},\ \mathbf{c}^{T(j)} \in \Re^{1x3},
\end{aligned} \tag{4}$$

with the matrix parameters

$$\begin{aligned}
&a_{21}^{(j)} = -k/m,\ a_{22}^{(j)} = -c/m,\ a_{23}^{(j)} = 2k_a \cdot x_{30}/(m \cdot k_b^2),\\
&a_{32}^{(j)} = x_{30}/k_b,\ a_{33}^{(j)} = -R \cdot k_b/(2\cdot k_a),\ b_{31}^{(j)} = k_b/(2\cdot k_a).
\end{aligned} \tag{5}$$

The variables in (4) are: $\Delta x_\gamma^{(j)} = x_\gamma^{(j)} - x_{\gamma 0}^{(j)}$, $\Delta y^{(j)} = y^{(j)} - y_0^{(j)}$, $j = \overline{1,6}, \gamma = \overline{1,3}$, representing the differences of the variables $x_\gamma^{(j)}$ and $y^{(j)}$ with respect to their values at the current operating point $P^{(j)}$, and referred to as $x_{\gamma 0}^{(j)}$ and $y_0^{(j)}$, respectively.

The transfer function (t.f) corresponding to Ln-Ms (4) has the general expression

$$\begin{aligned}
H_P^{(j)}(s) &= \mathbf{c}^{T(j)}(s\mathbf{I} - \mathbf{A}^{(j)})^{-1}\mathbf{b}^{(j)}\\
&= \frac{k_P^{(j)} / \prod_{\eta=1,3} p_\eta^{(j)}}{\prod_{\eta=1,3}(s - p_\eta^{(j)})} = \frac{k_{CP}^{(j)}}{\prod_{\eta=1,3}(1 + T_\eta^{(j)} s)},
\end{aligned} \tag{6}$$

where $k_{CP}^{(j)} = k_P^{(j)} / \prod_{\eta=\overline{1,3}} p_\eta^{(j)}$, $\mathbf{I}$ is the third-order identity matrix and the time constants of the plant are $T_\eta^{(j)} = -1/p_\eta^{(j)}, \eta = \overline{1,3}, j = \overline{1,6}$. The numerical values of the t.f.s. $H_P^{(j)}(s)$ at six operating points are synthesized in Table 1 (Dragos et al., 2012b).

3 DESIGN OF POSITION CONTROL SOLUTIONS

Four CSs are developed and analyzed as follows to obtain good performance of electromagnetic actuated clutch systems: PI controller and three PI gain-scheduling controllers.

Table 1: The numerical values of $H_P^{(j)}(s)$.

$P^{(j)}$, $j = \overline{1,6}$	$H_P^{(j)}(s),\ j = \overline{1,6}$
$P^{(1)}$	$\frac{0.3}{(1+0.064s)(1+0.016s)(1+0.0016s)}$,
$P^{(2)}$	$\frac{0.38}{(1+0.066s)(1+0.0164s)(1+0.0016s)}$,
$P^{(3)}$	$\frac{0.47}{(1+0.07s)(1+0.0162s)(1+0.0016s)}$,
$P^{(4)}$	$\frac{0.58}{(1+0.077s)(1+0.016s)(1+0.0016s)}$,
$P^{(5)}$	$\frac{0.745}{(1+0.087s)(1+0.0157s)(1+0.0016s)}$,
$P^{(6)}$	$\frac{0.9}{(1+0.098s)(1+0.0154s)(1+0.0016s)}$,

3.1 Design of PI Controllers

Depending on the operating points, six control solutions with PI controllers have been designed to ensure a small overshoot, offering an adequate phase margin ($\varphi_m = 60^\circ$) and a relatively small settling time.

The Modulus Optimum method is applied to initially tune the parameters of PI controllers (Åström and Hägglund, 1995):

$$H_{PI}^{(j)}(s) = k_c^{(j)}(1 + sT_c^{(j)})/s, \tag{7}$$

where $k_c^{(j)} = 1/(2 \cdot k_{CP}^{(j)} \cdot T_\Sigma^{(j)})$ is the controller gain, $T_c^{(j)} = T_1^{(j)}$ is the integral time constant. The numerical values of tuning parameters are: $k_c^{(1)} = 89$, $T_c^{(1)} = 0.064$, $k_c^{(2)} = 72.95$, $T_c^{(2)} = 0.066$ $k_c^{(3)} = 59.88$, $T_c^{(3)} = 0.07$, $k_c^{(4)} = 48.79$, $T_c^{(4)} = 0.077$, $k_c^{(5)} = 38.92$, $T_c^{(5)} = 0.087$ $k_c^{(6)} = 31.92$, $T_c^{(6)} = 0.098$.

The continuous PI controller (7) is discretized using Tustin's method with the sampling period T_s=0.003 s. Six discrete-time PI controllers with the following t.f.s are obtained:

$$H_{PI}^{(j)}(z^{-1}) = (q_0 + q_1 z^{-1})/(1 - z^{-1}), \tag{8}$$

where z^{-1} is the backward shift operator. The numerical values of tuning parameters are:

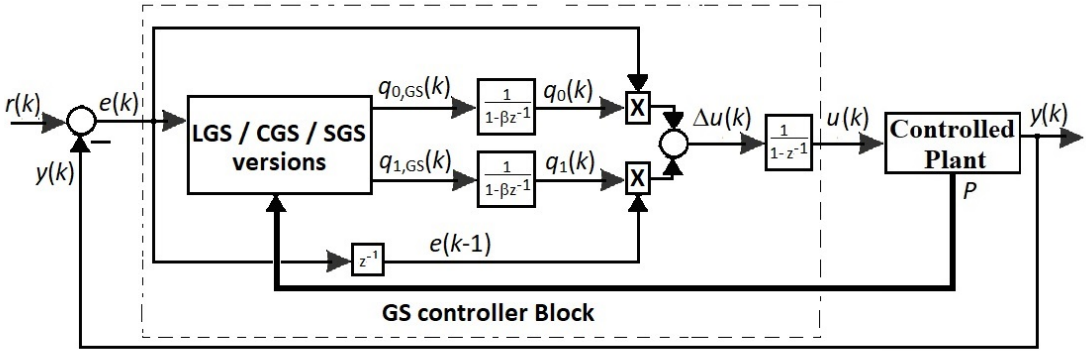

Figure 2: Schematic structure of the magnetically actuated mass-spring-damper system.

$q_0^{(1)} = 5.96$, $q_1^{(1)} = -5.70$, $q_0^{(2)} = 5.06$, $q_1^{(2)} = -4.82$, $q_0^{(3)} = 4.38$, $q_1^{(3)} = -4.20$, $q_0^{(4)} = 3.92$, $q_1^{(4)} = -3.77$, $q_0^{(5)} = 3.51$, $q_1^{(5)} = -3.40$, $q_0^{(6)} = 3.33$, $q_1^{(6)} = -3.23$.

3.2 Gain-scheduling Control Solutions Design

In order to ensure the switching between these six discrete PI controllers, three GS control solutions, namely Lagrange, Cauchy and Switching GS, Figure 2, are developed:

$$u(k) = u(k-1) + q_0(k)e(k) + q_1(k)e(k-1), \tag{9}$$

where k is the discrete time argument, $e(k)=r(k)-y(k)$ is the control error sequence, $y(k)$ is the process output sequence, $r(k)$ is the reference input sequence.

The discrete-time PI tuning parameters $q_{ik}, i \in \{0,1\}$ are

$$q_i(k) = \beta \cdot q_i(k-1) + q_{i,GS}(k), \tag{10}$$

extended or not with a first-order lag filter, where the parameter $\beta \in \{0, 0.1, 0.2, 0.3, 0.4, 0.5\}$ controls the transition speed between different controller parameters, and $q_{i,GS}(k)$ are regarded as reference inputs calculated as follows.

The proposed Lagrange GS (LGS) control solution is the first GS version, and it is based on a generalization to the multivariable case of the Lagrange interpolating parameter value method:

$$q_{i,LGS} = \sum_{j=1}^{n} \left(\frac{\alpha_{LGS}^{(j)}}{\sum_{j=1}^{n} \alpha_{LGS}^{(j)}} \cdot q_i^{(j)} \right), \quad i \in \{0,1\}, \tag{11}$$

where

$$\alpha_{LGS}^{(j)} = \prod_{l=0, l\neq j}^{n} \frac{\| P - P^{(l)} \|^2}{\| P^{(j)} - P^{(l)} \|^2}, \tag{12}$$

the superscripts j denote different operating points, $n = 7$, LGS is Lagrange GS version, $\| P - P^{(j)} \|$ is the Euclidean distance between the current operating point in the form of $P = (x_1, v, i_{EM1}, u_{EM1})^T$) and the nearest operating point $P^{(j)}$. All coefficients $\alpha_{LGS}^{(j)}$ in the first summation in (11) are normalized to add up to 1.

The Cauchy GS control solution is the second GS version which is based on a Cauchy kernel distance metric (Andonovski et al., 2016). This approach directly takes into account all previous data samples using :

$$q_{i,CGS} = \sum_{j=1}^{n} \left(\frac{\alpha_{CGS}^{(j)}}{\sum_{j=1}^{n} \alpha_{CGS}^{(j)}} \cdot q_i^{(j)} \right), \quad i \in \{0,1\}, \tag{13}$$

where

$$\alpha_{CGS}^{(j)} = \sum_{j=1}^{n} \frac{1}{1 + \| P - P^{(j)} \|^2}, \tag{14}$$

and *CGS* is Cauchy GS version, $\| P - P^{(j)} \|$ is the Euclidean distance between the current operating point *P* and the nearest operating point $P^{(j)}$.

The Switching GS (SGS) control solution is the third version. It is based on the switching between PI controllers and the PI controller parameters correspond to the nearest operating point during the real-time experiments. The selection is supported by the Euclidean distance metric resulting in

$$q_{i,SGS} = \sum_{j=1}^{n} \left(\frac{\alpha_{SGS}^{(j)}}{\sum_{j=1}^{n} \alpha_{SGS}^{(j)}} \cdot q_i^{(j)} \right),\ i \in \{0,1\}, \tag{15}$$

where

$$\begin{aligned} & q_{i,SGS} = q_i^{(j^*)}, \\ & j^* = \arg\min_{j=1,n} \| P - P^{(j)} \|^2,\ i \in \{0,1\}, \end{aligned} \tag{16}$$

and *SGS* is Switching GS version.

4 SIMULATION RESULTS

The proposed adaptive control structures presented above are tested and validated by six simulation results. A staircase change of the reference input signal was employed and the control structures responses were tested on the time frame of 10 s. The illustrated results include the evolutions of mass position $x_1(t)$ versus time *t* for Lagrange, Cauchy and Switching GS control solutions designed for the electromagnetic actuator as part of clutches system for $\beta \in \{0, 0.1, 0.2, 0.3, 0.4, 0.5\}$. Due to the lack of space, in this paper, only the results corresponding to $\beta = 0$, $\beta = 0.3$ and $\beta = 0.5$ are illustrated in Figures 3, 4 and 5.

The mean square error $\mathrm{J}_{\mathrm{MSE}_{\mathrm{GS}}}$ is computed for all three GS versions as:

$$\mathrm{J}_{\mathrm{MSE}_{\mathrm{GS}}} = \frac{1}{N} \sum_{t_d=1}^{N} (r(t_d) - y(t_d))^2, \tag{17}$$

where $\mathrm{GS} \in \{\mathrm{LGS}, \mathrm{CGS}, \mathrm{SGS}\}$ is the designed control solution, $r(t_d)$ is the reference input at time

Table 2: The mean square errors.

$\mathrm{J}_{\mathrm{MSE}_{\mathrm{GS}}}$	β					
	0	0.1	0.2	0.3	0.4	0.5
LGS	$8.52 \cdot 10^{-2}$	$8.12 \cdot 10^{-2}$	$7.72 \cdot 10^{-2}$	$7.33 \cdot 10^{-2}$	$6.94 \cdot 10^{-2}$	$6.57 \cdot 10^{-2}$
CGS	$8.31 \cdot 10^{-2}$	$7.93 \cdot 10^{-2}$	$7.55 \cdot 10^{-2}$	$7.17 \cdot 10^{-2}$	$6.80 \cdot 10^{-2}$	$6.44 \cdot 10^{-2}$
SGS	$8.68 \cdot 10^{-2}$	$8.28 \cdot 10^{-2}$	$7.89 \cdot 10^{-2}$	$7.51 \cdot 10^{-2}$	$7.14 \cdot 10^{-2}$	$6.77 \cdot 10^{-2}$

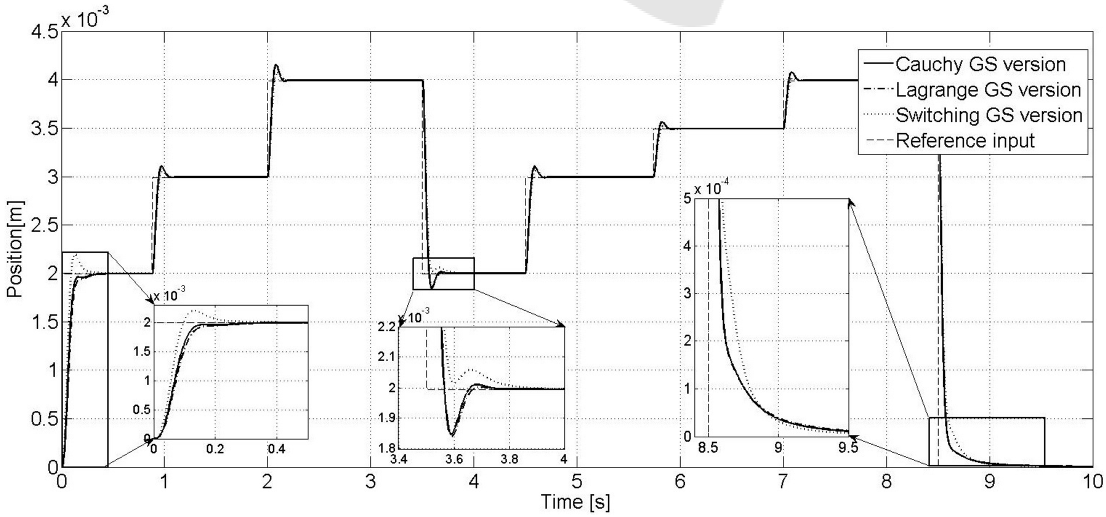

Figure 3: Mass position x_1 versus time (*t*) in all the three GS versions (namely CGS, LGS, SGS) for $\beta = 0$.

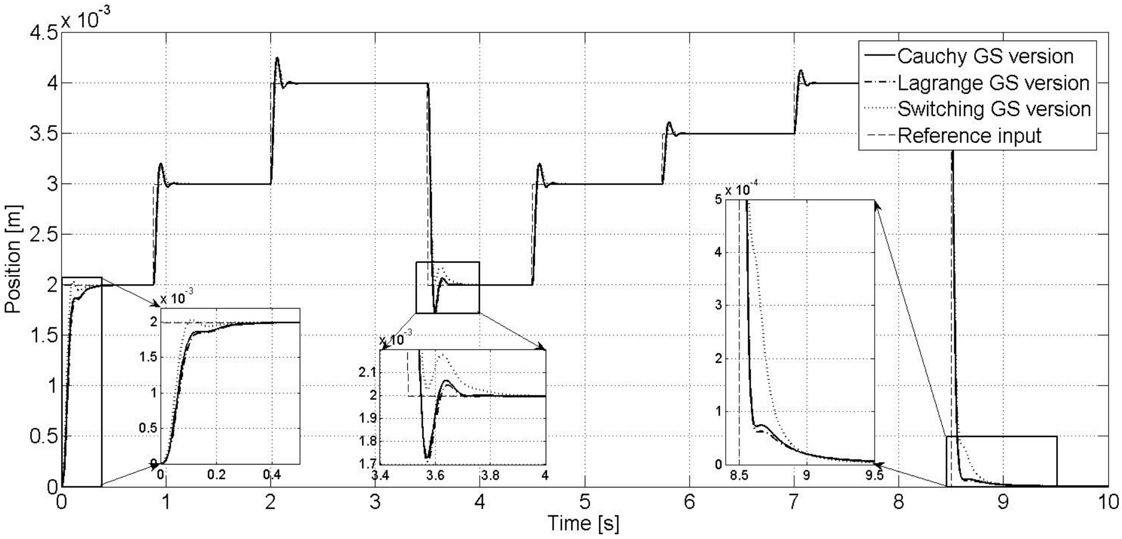

Figure 4: Mass position x_1 versus time (t) in all the three GS versions (namely CGS, LGS, SGS) for $\beta = 0.3$.

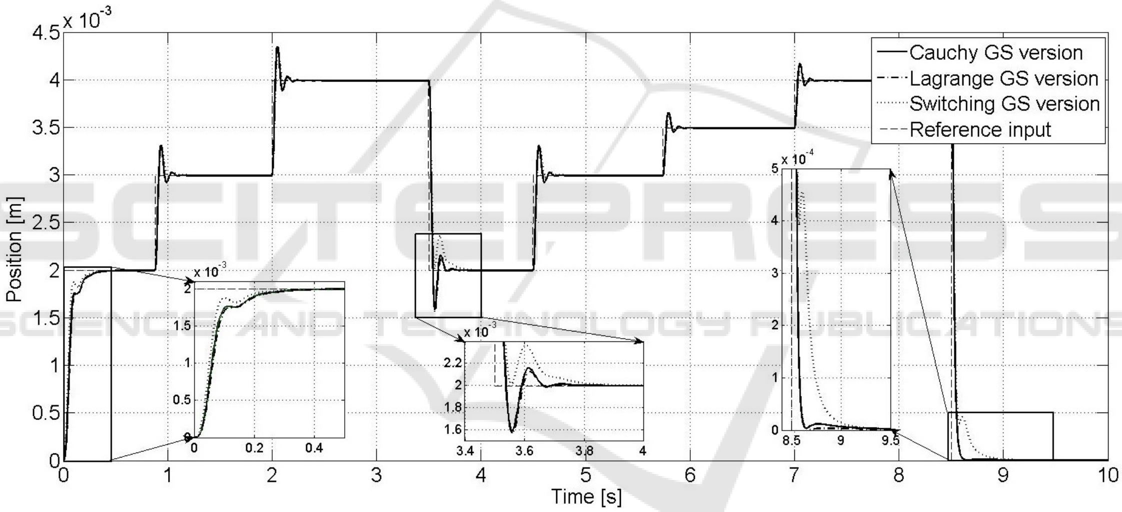

Figure 5: Mass position x_1 versus time (t) in all the three GS versions (namely CGS, LGS, SGS) for $\beta = 0.5$.

moment $t_d = 1...N$, N=3333 is the number of samples and $y(t_d)$ is the measured mass position at time moment t_d=1…N. The values are presented in Table 2.

The conclusion drawn by analyzing the plots given in Figures 3, 4 and 5, and after comparing the results presented in Table 2 is that the zero steady-state control error is ensured in all versions and the reference input is well tracked.

Analyzing in terms of GS versions the smallest mean square error is obtained in CGS version and the biggest mean square error is obtained in SGS version, and analyzing in terms of β the smallest mean square error is obtained for $\beta = 0.5$ and the biggest mean square error is obtained for $\beta = 0$ in all GS versions.

The above analysis of control system performance can lead to different results for other controlled plants. Such suggestive examples of plants include motion control (Korondi et al., 1996), chaotic systems (Precup et al., 2007), large-scale complex systems (Filip, 2008; Fan and Liu, 2016), multi-tank systems (Precup et al., 2013), evolving systems (Blažič et al., 2014), node localization (Derr and Manic, 2015; Wang et al., 2017), turbojet engines (Fozo et al., 2017), routing problems (Osaba et al., 2017) and neural networks (Dumitrache et al., 1999; Alique et al., 2000; Fioriti and Chinnici, 2017; Saadat et al., 2017;

Wagarachchi and Karunananda, 2017). Although they do not seem to be directly related to this paper, they point out the generality of GS approaches described in the previous sections.

5 CONCLUSIONS

This paper has presented the design of gain-scheduling control approaches viewed as adaptive control approaches developed to deal with the nonlinearities of the electromagnetic actuator and to ensure the switching between PI controllers. The simulation results prove that the GS-based control systems guarantee the performance improvement (zero steady-state control error, small settling times and small overshoots) with respect to staircase changes of the reference input.

Future research will be focused on the improvement of the performance indices by designing of CSs with PI(D) fuzzy gain-scheduling controllers, with model predictive controllers and hybrid structures applied to mechatronics systems.

REFERENCES

Alique, A., Haber, R. E., Haber, R. H., Ros, S., Gonzalez, C., 2000. Neural network-based model for the prediction of cutting force in milling process. A progress study on a real case. In *Proceedings of 15th IEEE International Symposium on Intelligent Control*. Patras, Greece, 121-125.

Andonovski, G., Blažič, S., Angelov, P., Škrjanc, I., 2015. Analysis of adaptation law of the robust evolving cloud-based controller, In *Proceedings of 2015 International Conference on Evolving and Adaptive Intelligent Systems*, Douai, France, 1-7.

Andonovski, G., Angelov, P., Blažič, S., Škrjanc, I., 2016. A practical implementation of robust evolving cloud-based controller with normalized data space for heat-exchanger plant. *Applied Soft Computing*. 48, 29-38.

Åström, K. J., Hägglund, T., 1995. *PID Controllers Theory: Design and Tuning*. Instrument Society of America, Research Triangle Park, NC, USA.

Bishop, R. H., 2008. *Mechatronic Systems, Sensors, and Actuators: Fundamentals and Modeling*. CRC Press, Boca Raton, FL, USA.

Blažič, S., Škrjanc, I., Matko, D., 2014. A robust fuzzy adaptive law for evolving control systems. *Evolving Systems*. 5 (1), 3-10.

Costa, B. S. J., Angelov, P. P., Guedes, L. A., 2015. Fully unsupervised fault detection and identification based on recursive density estimation and self-evolving cloud-based classifier, *Neurocomputing*. 150 (A), 289-303.

Derr, K. W., Manic, M., 2015. Wireless sensor networks - node localization for various industry problems. *IEEE Transactions on Industrial Informatics*. 11(3), 752-762.

Di Cairano, S., Bemporad, A., Kolmanovsky, I. V., Hrovat, D., 2007. Model predictive control of magnetically actuated mass spring dampers for automotive applications, *International Journal of Control*. 80, 1701-1716.

Dragos, C.-A., Precup, R.-E., Preitl, S., Petriu, E. M., Stinean, A.-I., 2012a. Takagi-Sugeno fuzzy control solutions for mechatronic applications, *International Journal of Artificial Intelligence*. 8 (S12), 45-65.

Dragos, C.-A., Preitl, S., Precup, R.-E., Petriu, E. M., Stinean, A.-I., 2012b. Adaptive control solutions for the position control of electromagnetic actuated clutch systems. In *Proceedings of 2012 IEEE Intelligent Vehicles Symposium*. Alcala de Henares, Spain, 81-86.

Dumitrache, I., Constantin, N., Drăgoicea, M., 1999. *Retele neurale: identificarea si conducerea proceselor*. Matrix Rom, Bucharest.

Fan, Z., Liu, X., 2016. Energy synchronized transmission control for energy-harvesting sensor networks. *International Journal of Computers Communications and Control*. 11 (21), 194-208.

Filip, F. G., 2008. Decision support and control for large-scale complex systems. *Annual Reviews in Control*. 32 (1), 61-70.

Fioriti, V., Chinnici, M., 2017. Node seniority ranking in networks. *Studies in Informatics and Control*. 26 (4), 397-402.

Fozo, L., Andoga, R., Beneda, K., Kolesár, J., 2017. Effect of operating point selection on non-linear experimental identification of iSTC-21v and TKT-1 small turbojet engines. *Periodica Polytechnica Transportation Engineering*. 45 (3), 141-147.

Gao, B., Chen, H., Liu, Q., Chu, H., 2014. Position control of electric clutch actuator using a triple-step nonlinear method, *IEEE Transactions on Industrial Electronics*. 61 (12), 6995-7003.

Haidegger, T., Kovács, L., Precup, R.-E., Benyó, B., Benyó, Z., Preitl, S., 2012. Simulation and control for telerobots in space medicine. *Acta Astronautica*. 181 (1), 390-402.

Korondi, P., Hashimoto, H., Gajdar, T., Suto, Z., 1996. Optimal sliding mode design for motion control. In *Proceedings of 1996 IEEE International Symposium on Industrial Electronics*. Warsaw, Poland, 277-282.

Losero, R., Guerra, T.-M., Lauber, J., Maurel, P., 2016. Electro-mechanical clutch actuator control based on output switched Takagi-Sugeno controller. *IFAC-PapersOnLine*, 49 (5), 85-90.

Oh, J. J., Choi, S. B., Kim, J., 2014. Driveline modeling and estimation of individual clutch torque during gear shifts for dual clutch transmission. *Mechatronics*. 24 (5), 449-463.

Osaba, E., Yang, X.-S., Diaz, F., Onieva, E., Masegosa, A., Perallos, A., 2017. A discrete firefly algorithm to solve a rich vehicle routing problem modelling a newspaper distribution system with recycling policy. *Soft Computing*. 21 (18), 5295-5308.

Precup, R.-E., Angelov, P., Costa, B. S. J., Sayed-Mouchaweh, M., 2015. An overview on fault diagnosis and nature-inspired optimal control of industrial process applications. *Computers in Industry*. 74, 75-94.

Precup, R.-E., David, R.-C., Petriu, E. M., 2017. Grey wolf optimizer algorithm-based tuning of fuzzy control systems with reduced parametric sensitivity. *IEEE Transactions on Industrial Electronics*. 64 (1), 527-534.

Precup, R.-E., Tomescu, M. L., Preitl, S., 2007. Lorenz system stabilization using fuzzy controllers. *International Journal of Computers Communications and Control*. 2 (3), 279-287.

Precup, R.-E., Tomescu, M. L., Preitl, S., Petriu, E. M., Fodor, J., Pozna, C., 2013. Stability analysis and design of a class of MIMO fuzzy control systems. *Journal of Intelligent and Fuzzy Systems*. 25 (1), 145-155.

Puig, V., Bolea, Y., Blesa, J., 2012. Robust fain-scheduled Smith PID controllers for second order LPV systems with time varying delay. *IFAC Proceedings Volumes*. 45(3), 199-204.

Ranjan, A., Prasanth, S., Cherian, F., Baskar, P., 2017. Design and control of electromagnetic clutch actuation system for automated manual transmission. *IOP Conference Series: Materials Science and Engineering*. 263, 1-13.

Saadat, J., Moallem, P., Koofigar, H., 2017. Training echo state neural network using harmony search algorithm. *International Journal of Artificial Intelligence*. 15 (1), 163-179.

Shamma, J. S., Athans, M., 1990. Analysis of gain scheduled control for nonlinear plants. *IEEE Transactions on Automatic Control*. 35 (8), 898-907.

Shin, Y. H., Kim, S. C., Kim, M. S., 2013. Use of electromagnetic clutch water pumps in vehicle engine cooling systems to reduce fuel consumption. *Energy*. 57, 624-631.

Temporelli, R., Micheau, P., Boisvert, M., 2017. Control of an electromechanical clutch actuator by a parallel adaptive feedforward and bang-bang controller: Simulation and experimental result. *IFAC-PapersOnLine*. 50 (1), 4787-4793.

Veselý, V., Ilka, A., 2013. Gain-scheduled PID controller design, *Journal of Process Control*. 23 (8), 1141-1148.

Wagarachchi, M., Karunananda, A., 2017. Optimization of artificial neural network architecture using neuroplasticity. *International Journal of Artificial Intelligence*. 15 (1), 112-125.

Wang, Y.-M., Zhang, F.-J., Cui, T., 2017. Fault diagnosis and fault-tolerant control for Manifold Absolute Pressure sensor (MAP) of Diesel engine based on Elman network observer. *Control Engineering and Applied Informatics*. 19 (2), 90-100.

Yang, Y.-N., Yan, Y., 2016. Attitude Regulation for Unmanned Quadrotors Using Adaptive Fuzzy Gain-scheduling Sliding Mode Control, *Aerospace Science and Technology*, 54, 208-217.